Advanced Palpation Sensor Systems Using PVDF Films

Mami Tanaka*

* Professor
Department of Biomedical Engineering, Graduate School of Biomedical Engineering
E-mail: mami@rose.mech.tohoku.ac.jp

Abstract

This paper is concerned with the development of advanced palpation sensor systems using PVDF (polyvinylidene fluoride) films as the sensory receptor and two topics are reported. One is the development of a tactile sensor to measure the stiffness of a living body which is considered applying to minimally invasive medical devices such as an endoscope and a catheter. The sensor to measure hardness was developed. Two sensors with different cylindrical columns were fabricated and their performance evaluation was conducted using silicone samples. The experimental results showed that the proposed tactile sensor can distinguish between samples on the basis of the elastic properties. The other is a fundamental research of the sensor for measuring touch sensation that should be effective for a palpation sensor. The touch feeling of 'Squeak-squeak' was focused. The sensory test and experiment by the developed sensor system were conducted. The results showed that there was high correlation between the time that the integrated sensor output to reach a threshold and sensory tests.

1. Introduction

The aging society with a declining birthrate is expected to cause many problems in the field of medical and welfare. The maintenance and improvement of QOL (quality of life) is effective to solve the problems. And the creation of QOL technology is important to maintain and improve QOL. The study of QOL technology should be considered not only from one field but from every field because the technology is for all people, such as, patients, elders, disabled people, caretakers, care receivers, physicians, people who care for someone, family members (people around care receivers) and others.

Under these circumstances, this paper reports a study on advanced palpation sensor system as a creation of QOL technology based on touch sensation and tactile sense in the medical and welfare engineering field. One part of the study is the development of a tactile sensor to measure the stiffness of a living body which is considered applying to minimally invasive medical devices such as an endoscope and a catheter. The other is fundamental research on measurement of a sense of 'Squeak-squeak (Kyu-kyu)' of human's tactile impression.

2. Development of an Endoscopic Tactile Sensor Using PVDF Films

Recently, minimally invasive surgery (MIS) has been used in the treatment of various diseases because it has many advantages including relief of pain, early recovery and small operative wounds. A catheter and/or endoscope are used during MIS. The operation of these tools is difficult because human cavities have a complex shape and it is hard for the operator to know the position/force information between the tools and human cavities. This difficulty might lead to a critical accident. To avoid undesirable results in MIS, the progression of endoscope technique is necessary. To ensure safe insertion, many studies have been performed, assessing an active endoscope with a shape memory alloy [1,2], a force sensor endoscope [3], and a sensor for monitoring the contact condition of an endoscope [4].

One of the disadvantages of MIS is the lack of tactile sensation. Information on tactile perception is important for the safety MIS and for diagnosis during MIS, but is not sufficient. To overcome this disadvantage, an endoscopic grasper with a tactile sensor [5] has been developed to manipulate biological tissue safely. Tanaka et al have developed an active palpation sensor using a polyvinylidene fluoride (PVDF) film to detect prostatic cancer and hypertrophy [6]. The PVDF film, used as the sensory material in the above studies, is a piezoelectric polymer material. It has good features, such as high sensitivity, lightweight, thin film, flexibility, and low cost. It also has the interesting feature that the output signal induced by an applied pressure is similar to the response of the Pacinian corpuscle, a sensory receptor in the human dermis, and is more sensitive to oscillatory pressure input [7]. In other words, in the case of applying a pressure pulse on PVDF, a brief potential signal is obtained at the up edge and down edge of the pulse, but there is no response to static pressure. Therefore, PVDF film is used to measure various tactile properties.

In this work, a tactile sensor using PVDF films was developed for endoscopic application. This sensor measures the hardness of biological tissue to assist with diagnosis. There are some indicative values of hardness. In this work, the elastic property, Young's modulus, is used to evaluate hardness. This sensor is composed of two PVDF films, a silicone cylindrical column and an

aluminum cylinder. The classification of Young's modulus is concerned with the ratio between these PVDF outputs. In this paper, two sensors are fabricated using two silicone cylindrical columns with different Young's moduli. The performance evaluation of each sensor was conducted using six silicone rubbers simulating the human prostate as measuring objects. The experimental results were compared with the theoretical analysis and the availability was confirmed.

3. Structure and Principle of the Tactile Sensor

A cross-section of the proposed tactile sensor is shown in Fig. 1. This sensor consists of two PVDF films, a cylindrical column of silicone rubber and a rigid aluminum cylinder attached to an aluminum block. The PVDF films are 28 μm in thickness. The silicone rubber is 3 mm in diameter and 3 mm in height. The aluminum cylinder is 6 mm in outer diameter, 4 mm in inner diameter and 3 mm in height. Aluminum blocks are 10 mm x 10 mm square and 3 mm in thickness. One of the PVDF films is laid under the silicone rubber; this film is called the upper PVDF. The other is sandwiched between the aluminum blocks and called the lower PVDF. Figure 2 shows a photograph of the prototype sensor. To reduce the overlap of noise, the connection between electrodes of PVDF and coaxial cables are shrouded by copper foil tape. In this study, two sensors, sensor H and sensor S, were fabricated using silicone rubbers with different Young's moduli. The Young's moduli of silicone rubbers used in sensors are shown in Table 1.

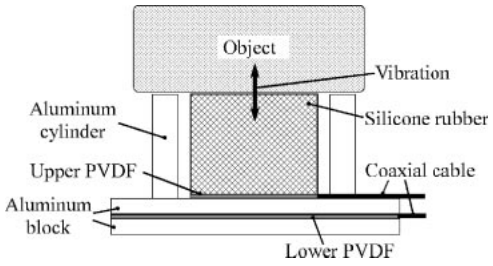

Fig. 1. Across-section of tactile sensor

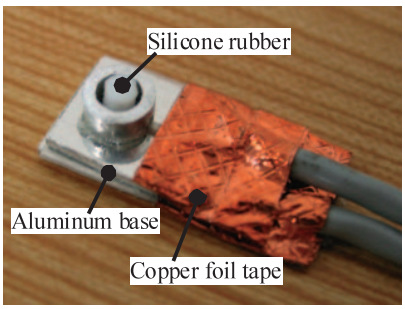

Fig. 2. Photograph of the tactile sensor

In measurements, PVDF output was obtained by vibrating the tactile sensor during contact with the object. When this sensor is pressed on the measuring object, forces F_a and F_s are applied on aluminum cylinder and silicone cylindrical column, respectively. The ratio between these forces depends on the Young's moduli of the aluminum, silicone rubber and measuring object. When a force is applied to a PVDF film, an electrical charge is induced by polarization in the PVDF film. Because the magnitude of its charge is proportional to the applied force, the applied force on a PVDF film can be obtained by measuring the output voltage through a charge amplifier connected to the PVDF film. The upper PVDF measures the force applied to the silicone rubber, F_s, and the lower PVDF measures the force applied to the whole sensor, namely, $F_a + F_s$. The ratio between these two PVDF outputs was calculated and the elastic property of the object being measured was determined.

Table 1. Young's modulus of the silicone column, E_s.

Sensor symbol	H	S
Young's modulus (MPa)	0.24	0.16

4. Theoretical Analysis

A theoretical model of the developed sensor is shown in Fig. 3. This modeling is based on some assumptions. One is that there is no shear force in either the measuring object or the sensor. Another is that the aluminum parts are considered as rigid bodies. It is also assumed that the surface of the measured object is flat. In the analytical model, A_a and A_s are the cross-sectional areas of the aluminum cylinder and the silicone rubber, respectively. T_o is the thickness of the measuring object. T_s is the thickness of the silicone cylindrical column and the aluminum cylinder. X_1 is the deformation of the measuring object on the rigid aluminum cylinder and X_2 is the deformation of the silicone cylindrical column. E_o and E_s are the Young's moduli of the measuring object and the silicone rubber, respectively. F_a and F_s are mentioned above, and force F is applied to the whole sensor. Using the theory of the mechanics of materials, these forces can be calculated from following equations.

$$F_a = E_o \frac{X_1}{T_o} A_a \qquad (1)$$

and

$$F_s = E_s \frac{X_2}{T_s} A_s = E_o \frac{X_1 - X_2}{T_o} A_s \qquad (2)$$

Combining the above expressions, we can obtain the ratio between the applied forces as

$$\frac{F_s}{F} = \frac{F_s}{F_a + F_s} = \frac{1}{\frac{A_a}{A_s}\left(1 + \frac{T_s E_o}{T_o E_s}\right) + 1} \qquad (3)$$

As mentioned in Sec. 2, F_s and F in equation (3) are measured by the upper PVDF film and the lower PVDF film, respectively. T_o, T_s, E_s, A_a and A_s are given. Then, we can calculate the Young's modulus of the measuring object, E_o. Fig. 4 shows the relationship between the force ratio, F_s/F, and the ratio between Young's moduli, E_o/E_s, using equation (3), designed to satisfy the conditions that A_s is equal to A_a and T_s is equal to T_o. When the measuring object is infinitely stiffer or softer than the silicone column, that is $E_o >> E_s$ or $E_o << E_s$, the ratio of forces asymptotically approaches zero or $A_s/(A_a+A_s)=0.5$. The force ratio changes significantly near $E_o/E_s=1$. In this case, a silicone rubber with stiffness near the measuring object is chosen as the sensor material for accuracy.

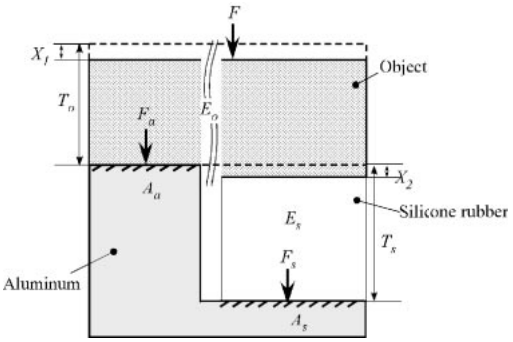

Fig. 3. An analytical model of the sensor and the measuring object.

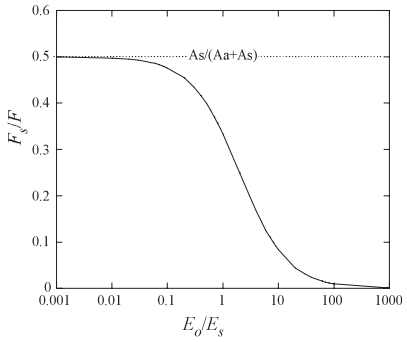

Fig. 4. A theoretical relationship between the force ratio and the ratio of Young's modulus E_o/E_s, in the case that $A_s=A_a$ and $T_s=T_o$.

5. Experiments

Figure 5(a) shows the experimental setup to confirm the performance of the developed tactile sensor. For simplicity, the sensor was fixed on the rigid table and the measuring object was attached to a vibro-machine. In this experiment, the measuring object was sinusoidally vibrated in the vertical direction by the vibro-machine. The amplitude and frequency of vibration were 2 mm and approximately 40 Hz, respectively. Maximum indentation depth was 0.5 mm. The upper and lower PVDF films were connected to each charge amplifier and a low-pass filter with a cut-off frequency of 1 kHz to remove the overlap of noises. Then, an oscilloscope collected the output signals for a measuring time 0.5 ms. The sampling frequency was 2.5 kHz. Six samples with different stiffnesses of silicone rubber were prepared as measuring objects. Each Young's modulus is summarized in Table 2. The stiffness was determined by considering the prostate gland. Sample A is the little softer than the stiffness of a cancerous prostate gland, and sample F was similar to the stiffness of healthy prostate gland[8]. Samples were 10 mm in thickness, width and length. Each sample was measured five times.

In addition, to take the practical use into account, experiments in which the measuring objects were fixed and the sensor was sinusoidally vibrated were conducted as shown in Fig. 5(b). In experiments, the same experimental setup was used except for cut-off frequency. The cut-off frequency of 45 Hz was chosen to reduce the noise due to vibration of the sensor.

Table 2. Young's modulus of sample objects, E_o.

Sample symbol	A	B	C	D	E	F
Young's modulus (MPa)	0.76	0.56	0.28	0.14	0.08	0.04

6. Results

Representative output waveforms from sensor S and sensor H are shown in Fig. 6 and 7, respectively. Panels (a) and (b) of each figure show the results for sample A. Panels (c) and (d) show the results for sample F. By comparison between samples, the sensor outputs for sample A were larger than those for sample F with both sensor S and sensor H. With regard to the

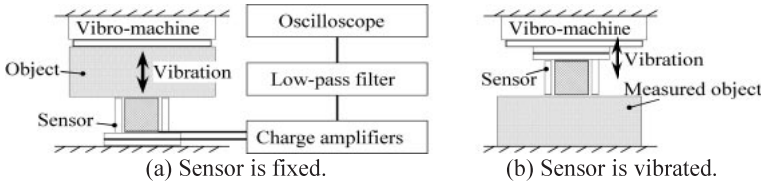

(a) Sensor is fixed. (b) Sensor is vibrated.

Fig. 5. Experimental setups in which (a) the sensor is fixed and the measuring object is vibrated, and (b) the sensor is vibrated and the measuring object is fixed. The same measurement system was used in all experiments.

comparison between the two sensors, although the output of the lower PVDF is unchanged, the outputs of the upper PVDF using sensor H are larger than those using sensor S.

The average amplitude $V_{p\text{-}p}$ was determined from each waveform. As $V_{p\text{-}p}$ of the upper PVDF and lower PVDF are described as V_{upper} and V_{lower}, respectively, V_{upper} is proportional to the force applied on the silicone cylindrical column, F_s, and V_{lower} is proportional to the force applied on the whole sensor, F. Therefore, the left side of equation (3) is represented as follows.

$$\frac{F_s}{F} = \frac{F_s}{F_a + F_s} = \frac{V_{upper}}{V_{lower}} \tag{4}$$

Using the above equation, the relationship between the experimental force ratio, F_s/F, and Young's modulus of the measuring object is shown in Fig. 8. The theoretical behaviors using equation (3) are also shown in Fig. 8. It was found that the experimental results with sensor H obviously corresponded with the simplified theoretical analysis. Also, in the case of sensor S, the experimental results roughly corresponded with the simplified theoretical ones, but the force ratio for harder samples grew larger than the theoretical one. In addition, by comparing the results with sensor H and sensor S, in both theoretical and

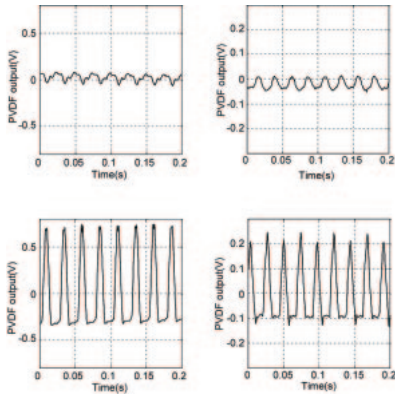

Fig. 6. The output waveforms of sensor S for sample A and F.

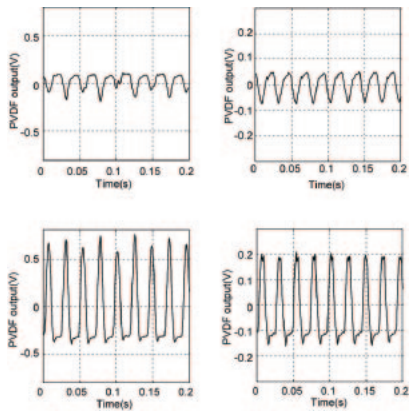

Fig. 7. The output waveforms of sensor H for sample A and F.

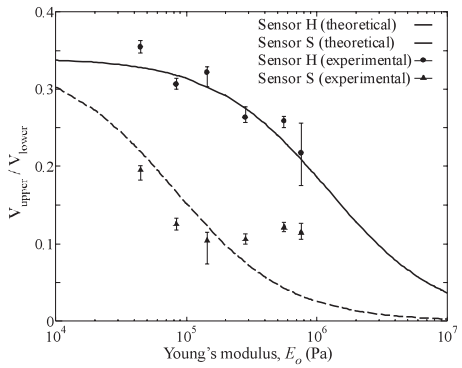

Fig. 8. Comparison between theoretical values and experimental results where the measured objects are vibrated.

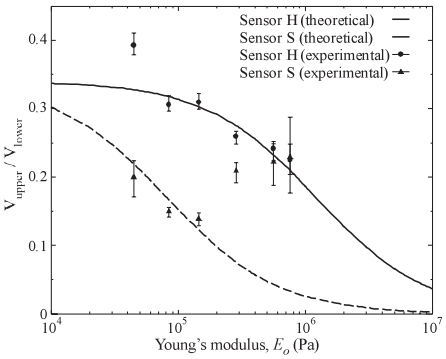

Fig. 9. Comparison between theoretical values and experimental results where the sensors are vibrated.

experimental results, it was confirmed that the classification performance depends on the Young's modulus of the cylindrical columnar material. The Young's modulus of the silicone cylinder can be determined by considering the threshold of classification. From these results, we confirmed that the proposed tactile sensor has enough availability to distinguish the hardness of the measurement object, including the biomedical tissue.

Next, Fig. 9 shows the results from a case in which the sensors are vibrated. With regard to sensor H, the experimental results corresponded with the theoretical results, and it is possible to discriminate a diseased prostate from a healthy one. In the results using sensor S, the measurements of harder samples disagreed with the theoretical curve, as shown in Fig. 8. In this case, it is impossible to discriminate between samples because the outputs for healthy and diseased prostates are the same. As the harder samples are measured by sensor S, the displacement of the silicone rubber of the sensor became larger and the effect of viscoelasticity or irregular deformation, including shear, torsion and bending deformation, became larger. To avoid irregular deformation, the machining accuracy of silicone rubber will need to be improved. For detailed design of sensors, we should conduct finite element analysis considering the viscoelasticity and shear force.

7. Development of a Tactile Sensor for Measuring Touch Sensation

From this chapter, the fundamental study of the sensor for measuring touch sensation that should be effective for a palpation sensor is reported.

When a dish that has been washed clean is rubbed with a finger, good tactile sense and a sound (vibration signal) like 'Squeak-squeak' (QQ) are obtained. A good detergent removes dirt cleanly and quickly, and can be washed off easily with tap water. The tactile sense is a slipping and stopping force when a finger moves across the surface of a dish or other object. The QQ feeling is defined as a combination of tactile sense and sound. Detergents that quickly give this QQ feel are considered to be good detergents. Therefore, the QQ feeling is one of the evaluation parameters a consumer considers when selecting a detergent. However, the QQ feeling depends on the tactile perception of the human finger, which is said to be ambiguous and subjective. This situation has drawn interest in the development of objective instrumentation that measures and evaluates the QQ feeling of dishes washed with different detergents. Tanaka and Tanaka et al developed the tactile sensors for measuring human touch sensation using PVDF films. The results show that PVDF film is useful as a receptor of a tactile sensor [9,10].

In this study, a tactile sensor system that can measure the quality of detergents is developed. In the experiment, a ceramic plate coated with various detergents is exposed to flowing water, and the plate is rubbed by a subject's finger. The times at which subjects obtained a QQ feeling were investigated as the sensory test. A tactile sensor using PVDF film as the receptor was fabricated. In experiments, the sensor scans the surface of the plate at regular intervals, with a similar procedure to the sensory test. To compare the results with those of the human sensory test, a threshold of integrated sensor output was set, and the time to reach the threshold was investigated. The times were compared with the results of the sensory test.

8. Sensory Test of QQ Feeling

The sensory test of QQ feeling was conducted with four subjects (I--IV) using four kinds of detergent(A--D). During the action of washing out each detergent, the times until subjects felt QQ were measured.

A detergent on a ceramic plate was used as a measurement object. The plate was washed with the same detergent before use to strip off any left-over material on the plate and to keep the same condition on the surfaces of the plates. A 3% solution of each detergent was prepared. These 3% samples were poured onto the centers of plates in 30-ml volumes and spread uniformly over the plates, which had a diameter of 10 cm. Plates were rinsed with water flowing from a tube positioned 1 cm above the center of the plate. The flow speed of the rinse water was 1.6 l/min. During rinsing, the subject rubbed the surface of the plate with a finger. The time until the subject felt QQ was measured. Each sample was evaluated five times by four subjects. The rinse water was 25 °C.

The results are presented in Table 3. The values in Table 3 are the average times from five trials with each sample evaluated by each subject. To reduce differences in sensitivity among individual subjects, the average time until subjects felt QQ for each sample was calculated and listed as the 'Average' in the table. The results show that all subjects felt QQ earlier using samples B and C than with the other samples, and that sample A required the most time for subjects to feel QQ.

Table 3. Time when subjects feel QQ feeling for each sample.

	Time(sec)				
	I	II	III	IV	Average
Sample A	17.59	19.67	19.63	20.26	19.29
Sample B	9.30	14.68	10.85	8.80	10.91
Sample C	3.82	8.72	6.62	9.26	7.1
Sample D	12.55	16.54	15.73	18.06	15.72

9. Tactile Sensor System and Signal Processing

The geometry of the tactile sensor is presented in Fig. 10. The sensor has a layered structure. The base of the sensor is an aluminum plate; a polyurethane rubber block and PVDF film, which are waterproofed with tarpaulin, are stacked in sequence. These are covered with rubber film with an uneven surface to increase the sensitivity of the sensor. All layers are bonded to each other by double-sided tape.

The experimental set up and measurement conditions are shown in Fig. 11 and Table 4, respectively. A ceramic plate was fixed on the Z axial slide table, and the sensor was fixed to the arm on the X axial slider. To contact the sensor, the plate was lifted up by the Z axial slide table, lifted a further 2 mm after theplate makes contact with the sensor to press the sensor onto the surface of the plate. The sliding direction of the sensor was parallel to the surface of the plate. The sensor slides on the surface of the plate using a stepping motor. The piezoelectric output of the PVDF film was digitized and stored by a personal computer.

Typical sensor outputs are presented in Fig. 12. In this figure, there are two peaks, one at the initiation of slipping and another at the end of slipping on the plate. The equivalent circuit for a PVDF film is depicted in Fig. 13. It is known that the open-circuit voltage (V_i in Fig. 13), which is immeasurable, is proportional to the pressure on the PVDF film and that the closed-circuit voltage (V_o in Fig. 13), which is measurable, is a differential transform of the open-circuit voltage. It follows that the open-circuit voltage, which depicts

pressure on the PVDF film [11], can be obtained by applying an integrated transform to the measured sensor outputs. Considering Fig. 13, *Vi* can be written as:

$$V_i(t) = V_o(t) * \left\{ \delta(t) + \frac{1}{RC} u(t) \right\} \qquad (5)$$

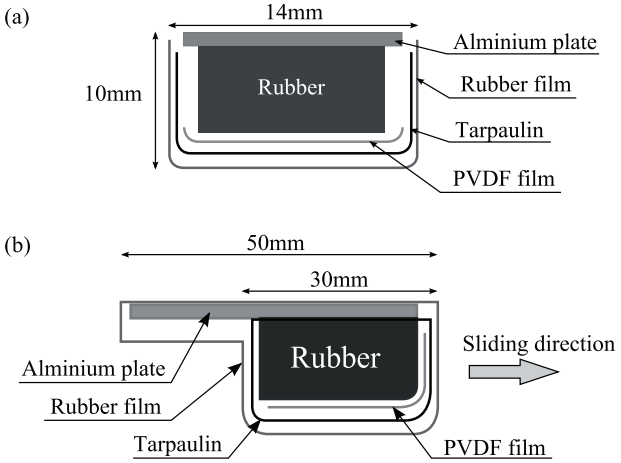

Fig. 10. Geometry of sensor: (a) Front view and (b) side view. Sliding direction of this sensor is right in (b).

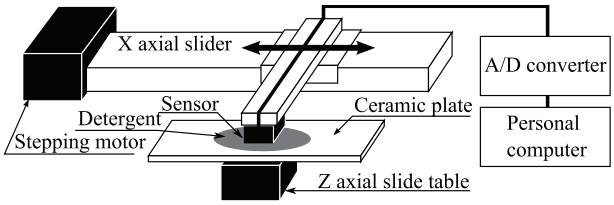

Fig. 11. Experimental set-up.

Table 4. Measurement conditions.

Sampling frequency	5 kHz
Measurement term	2 s
Sliding speed	50 mm/s
Sliding time	1 s

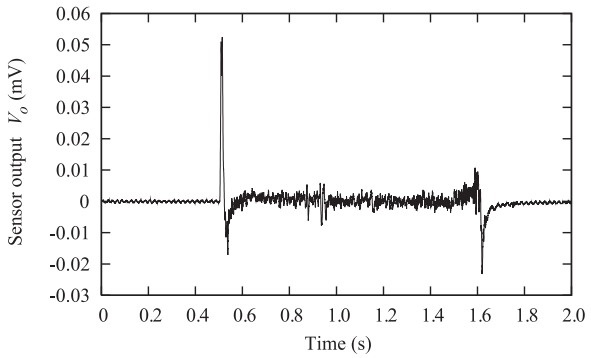

Fig. 12. An example of sensor output V_o.

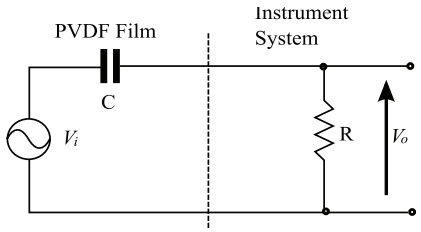

Fig. 13. Equivalent circuit for PVDF film.

Here, $\delta(t)$ is a delta function, $u(t)$ is a Heaviside unit function, * is the convolution integral, and t is the time from the start of measurement. In the experiment, *Vo* is measured in the form of discrete signals, as shown in Fig. 11. Therefore, V_i can be calculated from the following discrete form of Eq. (5).

$$V_i(n) = V_o(n) + \frac{T_s}{RC} \sum_{i=1}^{n} V_o(i) \qquad (6)$$

Here, T_S is the sampling period (0.2 ms), R is the resistance (1 MΩ), C is the capacitance of the PVDF film (1.38 nF) and n is the number of data points from the start of measurement. Applying Eq. (6) to the experimental data V_o, V_i is calculated and presented in Fig. 14. Considering that V_i is proportional to the pressure on the PVDF film, the value of peak 1 shown in Fig. 14 signifies the pressure on the PVDF film at the initiation of slipping. The value of peak 1 is defined as V_1, and the difference between peak 1 and peak 2 is defined as V_2. V_1 and V_2 were used to evaluate detergents as described below.

10. Sensor Measurement

10.1. Experiment 1

In experiment 1, the relationship between the amount of detergent remaining on a plate and the sensor output was investigated using four detergents (detergents A, B, C and D).

Table 5. Experimental conditions.

Air temperature	Water temperature	Humidity
17.9[°C]	17.5[°C]	52[%]

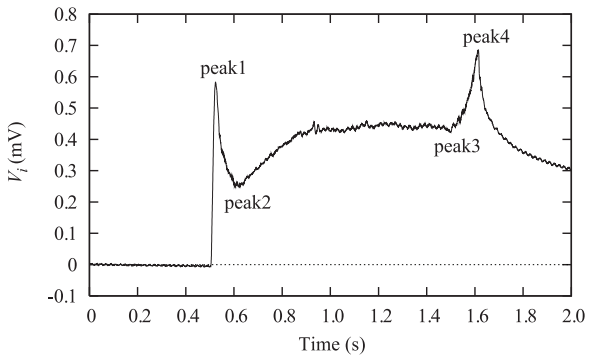

Fig. 14. Integrated sensor output V_i calculated by sensor output *Vo* of Fig. 12.

A ceramic plate was washed with the same detergent before use to strip off any left-over material on the plate and keep same condition of the surface of the plate. A 3% solution of each detergent was prepared, poured on the center of a plate by in a 30-ml volume, and spread uniformly over the plate making a diameter of 10 cm. The sensor was put on the plate 30 mm from the center, and sliding was commenced to collect sensor output. At the same time, the plate was rinsed with water from a tube positioned 1 cm above the center of the plate. The flow speed of the rinse water was 1 l/min. Measurement of sensor output was conducted every 10 s for 2 min. Samples were measured in triplicate, and the same procedure was repeated for all samples (sample A, B, C and D). The experimental conditions are shown in Table 5.

An example of sensor output is presented in Fig. 15. Each line in Fig. 15 is a time variation of the integrated sensor output. The result shows that V_1 and V_2 increase with time. To evaluate how V_1 and V_2 increase using each sample, thresholds were introduced. The threshold for V_1 was 0.8 and the threshold for V_2 was 0.5. The times T_1 and T_2 until V_1 and V_2 reached each threshold were measured for each sample. T_1 and T_2 values are shown in Table 6. T_1 and T_2 were small when using samples B and C, but large when using sample A.

Additionally, the coefficient between T_1 and T_2 is 0.953, T_1 and T_2 indicate a similar tendency.T_1 and T_2 were compared with the results of the sensory test described in section 2. The coefficient for the correlation between T_1 and the result of the sensory test was 0.95, and the coefficient for the correlation between T_2 and the result of the sensory test was 0.87. Thus there are strong correlations between the results of sensory tests by subjects and sensory experimental results.

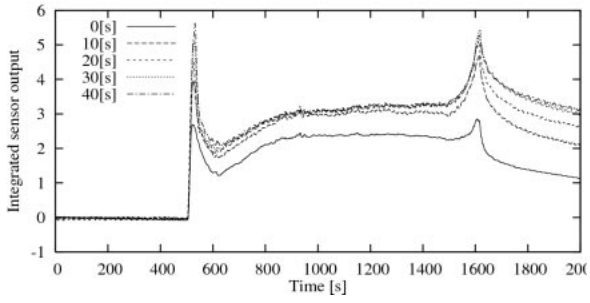

Fig. 15. An example of integrated sensor output V_i. Each line is the time variation of every 10 s.

Table 6. Time taken for V_1 and V_2 to reach each threshold using each detergent.

Time[s] \ Sample	A	B	C	D
T_1	60	10	10	30
T_2	50	10	20	40

Table 7. Time taken for V_1 and V_2 to reach each threshold using each detergent.

Detergent	A	B	C	D
Time[s]	40-60	0-10	0-10	20-40

Table 8. Experimental conditions.

Air temperature	Water temperature	Humidity
18.0 °C	14.9 °C	52 %

Table 9. T_1 and T_2 when the sensor scans every 1 s. Hyphen means no data (did not reach threshold).

	Time [s]							
	Threshold of V_1				Threshold of V_2			
Detergent	0.70	0.75	0.80	0.85	0.35	0.40	0.45	0.50
A	42	42	42	43	41	42	42	42
B	3	3	3	5	3	3	3	3
C	4	5	6	6	6	6	6	6
D	22	22	22	22	23	24	-	-

Table 10. Correlation coefficients of the T_1 and T_2 with the results of sensory tests for each threshold.

Threshold of V_1				Threshold of V_2			
0.70	0.75	0.80	0.85	0.35	0.40	0.45	0.50
0.92	0.93	0.93	0.95	0.94	0.93	0.92	0.92

10.2. Experiment 2

To more accurately determine T_1 and T_2, the measurement intervals applied in the experiment described in section 10.1 were narrowed. From the results described in section 10.1, T_1 and T_2 are in the time ranges shown in Table 7. The sensor scanned every 1 s during the intervals examined in this experiment.

The sensor slid on the surface of a plate every 10 s up to 2 min, and in the measurement time shown in the Table 5, the sensor scans every 1 s. The preparation and procedure for this experiment were the same as in experiment 1 in section 10.1 except for the measurement intervals and times. Here, this sensor system can't finish a series of operations within 1 s. To solve this problem, the flow of rinse water is stopped every 1 s, and the sensor scans again the surface of the plate. The experimental conditions are shown in Table 8.

To determine T_1 and T_2, six thresholds were added, and eight thresholds were set in total because V_1 reaches roughly 0.85 at the maximum. Four values were set as the thresholds of V_1 from 0.70 to 0.85. V_2 is less than 0.55, and some V_2 values measured using some samples were larger than 0.30 at the first scan. Thus four values were set as the thresholds of V_2 from 0.35 to 0.50. The set thresholds are shown by the top line in Table 9.

The results of this experiment are shown in Table 9. There are slight differences between the results using

each threshold. However, T_1 and T_2 correlate strongly with the results of the sensory tests described in section 2 (Table 10).

In addition, the value of peak 4 and the difference between peak 3 and peak 4 in Fig. 14 are defined as V_3 and V_4, respectively. The times until V_3 and V_4 reach the maximum are defined as T_3 and T_4, respectively. T_3 and T_4 were compared with the results of the sensory test. The coefficient of the correlation between T_3 and the result of the sensory test was 0.97, and the coefficient for the correlation between T_4 and the result of the sensory test was 0.98. There was also a strong correlation between V_3/V_4 and the results of sensory tests. These results show strong correlations between the QQ feeling and integrated sensor output, regardless of the value of the threshold.

11. Conclusion

This paper is concerned with the advanced palpation sensor systems using PVDF films and two topics are reported. One is the development of a tactile sensor measuring the stiffness of a living body considering the application to minimally invasive medical devices such as an endoscope and a catheter. The other is a fundamental research of the sensor for measuring touch sensation that should be effective for a palpation sensor. The obtained results can be summarized as follows.

1-1. A tactile sensor to measure hardness under an endoscope was developed using two PVDF films. Two sensors with different cylindrical columns were fabricated and their performance evaluation was conducted using silicone samples simulating the Young's modulus of the human prostate.

1-2. The experimental relationships between sensor output and the Young's modulus of the object roughly corresponded with the simplified theoretical ones. From the results it was found that the proposed tactile sensor can distinguish between samples on the basis of the elastic properties.

2-1.A sensor for the measuring human touch sensation was fabricated using PVDF film as the sensory material. As an application, the touch feeling of 'KYUKYU' was focused and the evaluation of detergents was conducted by the developed sensor system. Its validity for the sensor system was proven experimentally by using four detergents.

2-2.The time for the integrated sensor output to reach the threshold was found to have a high correlation with the results of sensory tests.

Acknowledgements

The author acknowledges the support of Tohoku University Global COE Program 'Global Nano-Biomedical Engineering Education and Research Network Centre'.

References

[1] Hirose S, Ikuta K, and Tsukamoto M. Developement of a shape memory alloy actuator. Measurement of material characteristics and development of active endoscopes. *Advanced Robotics* **4**, 3-27, 1990.

[2] Montesi MC, Martini B, Pellegrinetti A, Dario P, Lencioni L, and Montano A. An SMA-based flexible active endoscope for minimal invasive surgery. *Journal of Micromechanics and Microengineering* **5**, 180-182, 1995.

[3] Mosse CA, Mills TN, Bell GD, and Swain CP. Device for measuring the force exerted on the shaft of an endoscope during Colonoscopy. *Medical and Biological Engineering and Computing* **36**, 186-190, 1998.

[4] Tanaka M, Iijima T, Tanahashi Y, and Chonan S. Developmetn of 3D tactile sensor. *Journal of Material Processing Technology* **181**, 286-290, 2007.

[5] Najarian S, Dargahi J, and Zheng XZ. A novel method in measuring the stiffness of sensed objects with applications for biomedical robotic systems. *The international journal of medical robotics and computer assisted surgery* **2** ,84-90, 2006.

[6] Tanaka M, Furubayashi M, Tanahashi Y, and Chonan S. Development of an active palpation sensor for detection prostatic cancer and hypertrophy. *Smart Materials and Structures* **9**, 878-884 , 2000.

[7] Gordon M Shepherd, M.D., D Phil, *Neurobaiology.* Oxford University Press, Inc., New York, 215-221, 1998.

[8] Tanaka M, Cho J, Wang F, Chonan S, Chiba H, and Tanahashi Y. Optimum design of a prostate palpation sensor system. *Journal of Advanced Science* **17**, 46-48, 2005.

[9] Tanaka M. Development of tactile sensor for monitoring skin conditions. *Journal of Materials Processing Technology* **108**, 253-256, 2001.

[10]Tanaka M and Numazawa Y. Rating and valuation of human haptic sensation. *International Journal of Applied Electromagnetics and Mechanics* **19**, 573-579, 2004.

[11]Ikeda T. *Fundamental of Piezoelectricity*. Oxford University Press, New York, 1990.